The influence of the weak bond-energy dimerization on the single-particle optical conductivity of quasi-one-dimensional systems

Ivan Kupčić
Department of Physics, Faculty of Science, POB 331, HR-10 002 Zagreb, Croatia

The single-particle contributions to the optical conductivity of the quasi-one-dimensional systems has been reexamined by using the gauge-invariant transverse microscopic approach. The valence electrons are described by a model with the weak bond-energy dimerization, while the relaxation processes are taken into account phenomenologically. It turns out that the interband conductivity of the insulating half-filled case fits well the single-particle optical conductivity measured in various CDW systems. In the metallic regime, for the doubled Fermi vector $2k_{\rm F}$ close to π/a, the conduction electrons exhibit a non-Drude low-frequency response, with the total spectral weight shared between the intraband and interband channels nearly in equal proportions. For $2k_{\rm F}-\pi/a$ not to small, the behaviour of the conduction electrons can be described as the response of a simple Drude metal.

PACS numbers: 78.20.Bh,71.45.Lr
Keywords: Optical properties, CDW materials

I. INTRODUCTION

In recent years there has been a lot of experimental [1, 2, 3, 4, 5, 6, 7] and theoretical [8, 9, 10] interest in low dimensional systems which exhibit a gap (for T below the critical temperature T_c) or pseudogap ($T > T_c$) features in the low-frequency optical conductivity. In principle, it is possible to solve the single-particle contributions to the response functions for the ideal electronic system and then to take the single-particle damping phenomenologically. However, a good agreement with experiments cannot be achieved by such phenomenological extension of the standard transverse microscopic theory, which was the question raised by Kim at al. [8]. Instead, they developed a more rigorous method which fits well the single-particle conductivity in various quasi-one-dimensional (Q1D) systems with the CDW instability.

Surprisingly, a straightforward calculation gives that the longitudinal microscopic response theory, with the phenomenologically treated disorder, also agrees with the single-particle optical conductivity measured in the CDW systems [11]. The origin of the inconsistency between two microscopic approaches represents an interesting question which will be examined in the present paper. The purpose of the paper is threefold; first, to determine the gauge-invariance requirement for the electronic systems with the bond-energy dimerization (by considering the simplest case); second, to argue that in the weak-splitting limit the dielectric function has the usual form, at variance with the conclusions of the analysis based on the electric-dipole approximation [12] that the dielectric function has the Lorentz-Lorenz form even in this limiting case; finally, to illustrate that in the weak-splitting limit various Drude-like and non-Drude low-frequency metallic behaviours are possible.

In this paper, we shall consider the electronic system stabilized into an ordered phase described by the wave vector $Q = \pi/a$. It will be assumed that Q differs from the doubled Fermi vector, $2k_{\rm F}$, leading to a metallic state with the bond-energy dimerization. Such assumption is natural, in particular in the strong-splitting case, describing primarily the molecular crystals with an important role played by the local field corrections. According to Refs. [13, 14], the weak-splitting $Q \neq 2k_{\rm F}$ microscopic model should also be interesting. The optical conductivity obtained in this case is expected to be relevant to the CDW systems, both at $T < T_c$ and $T > T_c$, but for the frequencies well above the frequency of the pinned collective mode.

In Sec. 2 we determine the optical conductivity $\sigma_\alpha^{\rm total}(\omega)$ and the associated dielectric function in the Q1D model with the weak bond-energy dimerization, taking properly into account gauge invariance of the response theory. Sec. 3 illustrates that the gauge invariance enables the rigorous treatment of the effective mass theorem (and the associated effective number of conduction electrons), as well as of the conductivity sum rules. Additionally, it is explained how the standard transverse treatment of the interband optical processes [15, 16] can be remedied. The development of $\sigma_x^{\rm total}(\omega)$ with doping is shown for a few characteristic cases. Finally, the concluding remarks are given in Sec. 4.

II. THEORETICAL MODEL

We consider the Q1D electronic system with the bond-energy dimerization along the x axis in the presence of the electromagnetic fields. The Hamiltonian reads as

$$\begin{aligned} H &= \sum_{n\sigma}[t_>\tilde\beta^\dagger_{n\sigma}\tilde\alpha_{n\sigma} + t_<\tilde\alpha^\dagger_{n+2a\sigma}\tilde\beta_{n\sigma} \\ &\quad + t_b(\tilde\alpha^\dagger_{n+b\sigma}\tilde\alpha_{n\sigma} + \tilde\beta^\dagger_{n+b\sigma}\tilde\beta_{n\sigma}) + \text{H.c.}], \end{aligned} \tag{1}$$

where the influence of the external fields is introduced through

$$\tilde l^\dagger_{n\sigma} = l^\dagger_{n\sigma} e^{{\rm ie}/(\hbar c)(\mathbf{R}_n+\mathbf{r}_l)\cdot\mathbf{A}(\mathbf{R}_n+\mathbf{r}_l)}, \tag{2}$$

and where $l^{\dagger}_{n\sigma}$, $l \in \{\alpha, \beta\}$, is a creation operator on the $\mathbf{R}_n + \mathbf{r}_l$ site. In order to preserve a simple form of the intracell phase factors, we approximate the positions of atoms within the unit cell of the dimerized case with their positions in the original lattice (for example, $r_{\alpha x} = 0$ and $r_{\beta x} = a$, with $\mathbf{a}_1 = a\hat{\mathbf{x}}$ and $\mathbf{a}_2 = b\hat{\mathbf{y}}$ representing the primitive vectors of the original lattice). For the bond energies we assume that $t_i < 0$ and $|t_>| > |t_<| > |t_b|$, i.e., the x axis represents the strong axis of the present Q1D system.

In principle, it is possible to generalize the theory to include all relevant relaxation processes explicitly. Instead, we adopt an approach which assumes that in the clean (i.e. underdamped) limit one can separate the relaxation of the electron momentum on the static dimerization potential (or on the (quasi)static $Q = \pi/a$ phonon modes) from other electron scattering processes (related to the impurities and other phonon modes), calculate the dimerization (or (quasi)dimerization) effects exactly, and, finally, take the remaining relaxation effect into account phenomenologically.

A. Bare Hamiltonian

The Bloch operators of the dimerized case satisfy the relation

$$L^{\dagger}_{\mathbf{k}\sigma} \;=\; \frac{1}{\sqrt{N}} \sum_n e^{\mathrm{i}\mathbf{k}\cdot\mathbf{R}_n} \sum_l e^{\mathrm{i}k_x r_{lx}} U_{k_x}(L,l) l^{\dagger}_{n\sigma}, \tag{3}$$

where $e^{ik_x r_{lx}}$ are the bare intracell phase factors, and where $U_{k_x}(L,l)$ represent the transformation-matrix elements dependent on an additional phase $\varphi(k_x)$, as discussed below. For $t_i < 0$, the band indices $L = S$ and $L = A$ stand for the lower (symmetric) and upper (antisymmetric) band, respectively. It is also assumed that the lower band is partially filled and the upper band is empty. If the Fermi level is in the upper band, the following expressions remain the same, only the electron picture has to be replaced by the hole picture.

Inserting $\mathbf{A}(\mathbf{R}_n + \mathbf{r}_l) = 0$ in Eqs. (1) and (2), we obtain the bare Hamiltonian H_0. After diagonalization, this Hamiltonian becomes

$$H_0 \;=\; \sum_{\mathbf{k}\sigma L} E_L(\mathbf{k}) L^{\dagger}_{\mathbf{k}\sigma} L_{\mathbf{k}\sigma}. \tag{4}$$

The Bloch energies are given by

$$E_{A,S}(\mathbf{k}) \;=\; E_b(k_y) \pm E_a(k_x), \tag{5}$$

where

$$\begin{aligned} E_b(k_y) \;&=\; -2|t_b| \cos k_y b, \\ E_a(k_x) \;&=\; \sqrt{\varepsilon^2(k_x) + \Delta^2(k_x)}. \end{aligned} \tag{6}$$

The corresponding transformation-matrix elements are

$$\begin{aligned} &\begin{pmatrix} U_{k_x}(S,\alpha) & U_{k_x}(S,\beta) \\ U_{k_x}(A,\alpha) & U_{k_x}(A,\beta) \end{pmatrix} = \\ &= \frac{\sqrt{2}}{2} \begin{pmatrix} e^{\mathrm{i}\varphi(k_x)/2} & e^{-\mathrm{i}\varphi(k_x)/2} \\ e^{\mathrm{i}\varphi(k_x)/2} & -e^{-\mathrm{i}\varphi(k_x)/2} \end{pmatrix}, \end{aligned} \tag{7}$$

where the auxiliary phase $\varphi(k_x)$ satisfies the p-symmetry-gap relation

$$\tan\varphi(k_x) \;=\; \frac{\Delta(k_x)}{\varepsilon(k_x)}. \tag{8}$$

Other notation is given by

$$\begin{aligned} \varepsilon(\mathbf{k}) \;&=\; 2|t_a| \cos k_x a, \\ \Delta(\mathbf{k}) \;&=\; \Delta_0 \sin k_x a, \end{aligned} \tag{9}$$

with $2|t_a| \equiv |t_>| + |t_<|$ being the averaged intrachain bond energy and $\Delta_0 \equiv |t_>| - |t_<|$ is the magnitude of the gap function.

One recognizes in Eqs. (3) and (7) the total intracell phases of the form $\Phi_\alpha(k_x) = k_x r_\alpha + \varphi(k_x)/2$, for the $|\alpha n\rangle$ states, and $\Phi_\beta(k_x) = k_x r_\beta - \varphi(k_x)/2$, for the $|\beta n\rangle$ states. At this point it is interesting to note that if we take the strong-splitting limit, where $\Delta_0/(2|t_a|) \approx 1$, we obtain $\varphi(k_x) \approx k_x a$, and finally $\Phi_\alpha(k_x) \approx \Phi_\beta(k_x)$. Such structure of the intracell phases suggests the usage of the molecular representation, based on the molecular orbitals $1/\sqrt{2}(|\alpha n\rangle \pm |\beta n\rangle)$, with a further electric-dipole approximation (for example, see Ref. [12]). In the weak-splitting limit, however, the atomic $|ln\rangle$ representation is more adequate, as argued in the below discussion of the interband current vertices.

B. Electron-photon coupling

In order to write explicitly all relevant electron-photon coupling functions, we need the Taylor expansion in the vector potential of Eq. (1) to the second order. The first-order term and the direct second-order term become

$$\begin{aligned} H_1^{\mathrm{ext}} \;&=\; -\frac{1}{c} \sum_{\mathbf{k}\sigma} \sum_{LL'} \sum_i [A_{x_i}(\mathbf{q}_{\perp i}) J_{x_i}^{LL'}(\mathbf{k}) \\ &\quad \times L^{\dagger}_{\mathbf{k}+\mathbf{q}_{\perp i}\sigma} L'_{\mathbf{k}\sigma} + \mathrm{H.c.}], \\ H_2^{\mathrm{ext}} \;&=\; \frac{e^2}{2mc^2} \sum_{\mathbf{k}\sigma} \sum_{LL'} \sum_i [A^2_{x_i}(\mathbf{q}_{\perp i}) \gamma_{x_i x_i}^{LL'}(\mathbf{k};2) \\ &\quad \times\; L^{\dagger}_{\mathbf{k}+\mathbf{q}_{\perp i}\sigma} L'_{\mathbf{k}\sigma} + \mathrm{H.c.}], \end{aligned} \tag{10}$$

respectively, with $x_i \in \{x, y\}$. Furthermore, $A_{x_i}(\mathbf{q}_{\perp i})$ and $A^2_{x_i}(\mathbf{q}_{\perp i})$ represent the Fourier transforms of $A_{x_i}(\mathbf{r})$ and $A^2_{x_i}(\mathbf{r})$, and $\mathbf{q}_{\perp i} \cdot \mathbf{a}_i = 0$. The explicit form of the coupling functions, the current vertices $J_{x_i}^{L_1 L_2}(k_i)$ and the bare Raman vertices $\gamma_{x_i x_i}^{L_1 L_2}(k_i;2)$, is given in the Appendix.

It is essential to notice that in the bond-energy dimerization model two physically different terms comprise the interband current vertices. The first term is dispersionless and corresponds to the intramolecular interband processes (between the states $|\alpha n\rangle$ and $|\beta n\rangle$). The second term describes all other, intermolecular interband processes. In the strong-splitting limit, one obtains the interband current vertices consisting mainly of the intramolecular contribution, $J_x^{SA}(k_x) \approx \mathrm{i}ea|t_>|/\hbar$, giving the associated dipole vertex of the form $ea/2$. Although in this case the response functions are complicated functions of the short-range dipole-dipole interactions, it is possible to apply the electric-dipole approximation, and to obtain the Q1D optical model extensively studied by Županović at al. [12]. In the present article we want to extract physical information from the optical conductivity determined in the opposite (weak-splitting) limit. In this case the intramolecular and intermolecular interband processes are equally important, and, consequently, the local field corrections become negligible.

C. Optical conductivity in the weak-splitting limit

To obtain the gauge invariant form of the (transverse) optical conductivity in the ideal multiband models, it is necessary first to gather the diamagnetic photon self-energy with the real part of the static interband photon self-energies [17, 18]. This results in the effective mass theorem [10]

$$[m^{SS}_{x_ix_i}(k_{x_i})]^{-1} = \frac{1}{m}\gamma^{SS}_{x_ix_i}(k_{x_i}) = \frac{1}{m}\gamma^{SS}_{x_ix_i}(k_{x_i};2) - \frac{2|J^{SA}_{x_i}(k_{x_i})|^2}{e^2E_{AS}(k_x)}. \quad (11)$$

Here $E_{AS}(k_x) = E_A(\mathbf{k}) - E_S(\mathbf{k}) = 2E_a(k_x)$. $\gamma^{SS}_{x_ix_i}(k_{x_i})$ is the static Raman vertex, which can also be written in the form $(m/\hbar^2)\partial^2 E_S(\mathbf{k})/\partial k^2_{x_i}$ [19]. When the local field corrections are absent for the symmetry reasons, or are negligible, the remaining contributions to the total photon self-energy lead to the ideal intraband and interband optical conductivities given by

$$\sigma^{\mathrm{intra}}_{x_i}(\omega,\eta_1) = \frac{\mathrm{i}}{\omega}\frac{e^2n^{\mathrm{eff}}_{x_i}}{m}\frac{\hbar\omega}{\hbar\omega+\mathrm{i}\eta_1}, \quad (12)$$

$$\sigma^{\mathrm{inter}}_{x_i}(\omega,\eta_2) = \frac{\mathrm{i}}{\omega}\frac{1}{V}\sum_{\mathbf{k}\sigma}\frac{(\hbar\omega)^2|J^{SA}_{x_i}(k_{x_i})|^2}{E^2_{AS}(k_{x_i})} \times\left\{\frac{f_S(\mathbf{k})}{\hbar\omega - E_{AS}(k_{x_i})+i\eta_2} - \frac{f_S(\mathbf{k})}{\hbar\omega + E_{AS}(k_{x_i})+\mathrm{i}\eta_2}\right\}, \quad (13)$$

respectively. The effective number of conduction electrons can be shown as an integral of the static Raman vertex over all occupied states [2, 20],

$$n^{\mathrm{eff}}_{x_i} = \frac{1}{V}\sum_{\mathbf{k}\sigma}\gamma^{SS}_{x_ix_i}(\mathbf{k})f_S(\mathbf{k}), \quad (14)$$

or as an integral of the square of the electron group velocity over the Fermi surface,

$$n^{\mathrm{eff}}_{x_i} = m\frac{1}{V}\sum_{\mathbf{k}\sigma}|v_{x_i}(k_{x_i})|^2\delta[E_S(\mathbf{k})-\mu], \quad (14')$$

(notice that for the free electrons both of these expressions reduce to the total number of conduction electrons). Here $f_S(\mathbf{k})$ is the abbreviation for the Fermi-Dirac function $f[E_S(\mathbf{k})]$. Furthermore, notice that the expressions (12) and (13) describe the case of a normal photon incidence, $\mathbf{A}(\mathbf{r}) = (A_x(y), 0)$, or the case of the parallel photon incidence, $\mathbf{A}(\mathbf{r}) = (0, A_y(x))$. The generalization of these expressions is straightforward, and will be briefly discussed below.

It is rather a good approximation to treat the single-particle damping (connected with the impurities and the remaining phonons) phenomenologically, by replacing the adiabatic terms η_j with the corresponding damping energies Σ_{jx_i}. Then the total conductivity becomes

$$\sigma^{\mathrm{total}}_{x_i}(\omega) = \sigma^{\mathrm{intra}}_{x_i}(\omega,\Sigma_{1x_i}) + \sigma^{\mathrm{inter}}_{x_i}(\omega,\Sigma_{2x_i}). \quad (15)$$

Finally, we obtain that the associated dielectric function reads as

$$\varepsilon_{x_i}(\omega) \approx \varepsilon_\infty + \frac{4\pi\mathrm{i}}{\omega}\sigma^{\mathrm{total}}_{x_i}(\omega). \quad (16)$$

The contributions of the high-frequency optical processes, not included in Eq. (1), are assumed to be constant up to frequencies well above the considered frequency region, and are represented by $\varepsilon_\infty - 1$.

III. RESULTS AND DISCUSSION

In the weak-splitting conductivity (15), $2|t_a|$ is the largest parameter of the model. In spite of the phenomenological description of the single-particle damping, this expression is a rather complicated function of the remaining parameters, $2|t_b|$, $k_{\mathrm{B}}T$, Σ_i and $E_{AS}(\mathbf{k}_{\mathrm{F}})$ (the dependence of $\sigma^{\mathrm{total}}_{x_i}(\omega)$ on the parameter $2\mathbf{k}_{\mathrm{F}} - \mathbf{Q}$ is represented here through the bare interband threshold energy $E_{AS}(\mathbf{k}_{\mathrm{F}})$) which makes further rigorous analytic treatment very difficult. In this respect, we shall limit the below discussion only on some simple limiting cases.

A. Strictly 1D limit

If the electronic system is treated as strictly one-dimensional, i.e. $|t_b| = 0$, one obtains that the electron

dispersion in the perpendicular direction, $E_b(k_y)$, vanishes. Similarly, for the incidence of the electromagnetic fields normal to the chains, the probability of the photon absorption (or emission) disappears, as well. In this case, the real part of the conductivity comprises only the $\delta(\omega)$ term, corresponding to the elastic photon scattering. According to the effective mass theorem (11), the coupling constant arises from two mutually competing terms, the diamagnetic term and the static contributions in the interband term, and is given by the $\eta_1 \to 0$ limit of (12), with $n_{x_i}^{\rm eff}$ given by (14). For non-normal incidence, the effective number of conduction electrons, $n_x^{\rm eff}$, has to be replaced by $\sin^2\varphi\, n_x^{\rm eff}$, where φ is the angle between $\mathbf{A}(\mathbf{r})$ and $\hat{\mathbf{x}}$. In this way, one can derive the well-known anisotropic dispersion of the longitudinal plasma modes. Namely,

$$\sigma_x^{\rm intra}(\omega) \;\approx\; \frac{\mathrm{i}}{\omega}\frac{e^2 n_x^{\rm eff}}{m}\sin^2\varphi, \tag{17}$$

and finally

$$\omega_{\rm pl}^2(\mathbf{q}) \;\approx\; \frac{4\pi e^2 n_x^{\rm eff}}{\varepsilon_\infty m}\frac{q_x^2}{q_x^2+q_y^2}. \tag{18}$$

To proceed with the numerical calculation, we will take the conductivity (15) in the usual Q1D limit, $|t_a| \gg |t_b| \neq 0$ (hereafter this limit is denoted by $|t_b| \to 0$). In the optical conductivity considerations concerned only with the single-particle contributions, the "explicit" influence of the interchain hopping processes on Eq. (15), through the Bloch energies, can be neglected. Nevertheless, these processes will be taken into account implicitly, since they lead to a finite probability of the photon absorption (emission). In such circumstances the 1D version of Eq. (15), with the non-zero damping energies, can safely be used. Furthermore, we restrict the analysis on the case of normal photon incidence, where only the $x_i = x$ conductivity is non-zero. We also assume that $\Sigma_1 = \Sigma_2 \equiv \Sigma$ and $\mathbf{k}_{\rm F} = k_{\rm F}\hat{\mathbf{x}}$.

B. Gauge invariance

The gauge invariance of the conductivity (15) can be easily proved term by term, by the direct calculation of the longitudinal dielectric function, following the procedure developed in Refs. [20] and [10]. The most important qualitative consequences of the gauge-invariance requirement are as follows.

Fig. 1 shows the influence of the dimerization on the (normalized) optical conductivity in the most interesting metallic case ($k_{\rm F} = 0.475\pi/a$), where the $T \approx 0$ K total spectral weight is shared between the intraband and interband contributions nearly in equal proportions. The participation of the intraband (i.e. Drude) part in the total spectral weight raises significantly with increasing temperature. On the other hand, the temperature dependence of the dc conductivity $\sigma_x^{\rm dc} \equiv {\rm Re}\{\sigma_x^{\rm total}(0)\}$ results

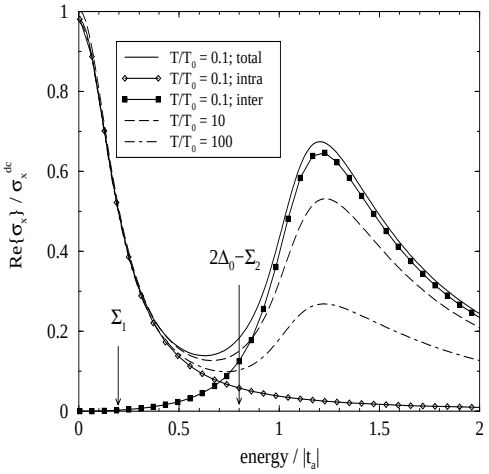

FIG. 1: The explicit temperature dependence of the real part of the optical conductivity for $|t_b| \to 0$, $\Delta_0 = 0.5|t_a|$, $\Sigma = 0.2|t_a|$, and $k_{\rm F} = 0.475\pi/a$. The temperature scale T_0 is given by $k_{\rm B}T_0 = 10^{-3}\cdot 2|t_a|$ (for example, $T_0 \approx 4$ K, $\Delta_0 \approx 0.1$ eV and $\Sigma \approx 0.04$ eV, for $|t_a| \approx 0.2$ eV). The intraband and interband contributions at $T = 0.1T_0$ are also shown.

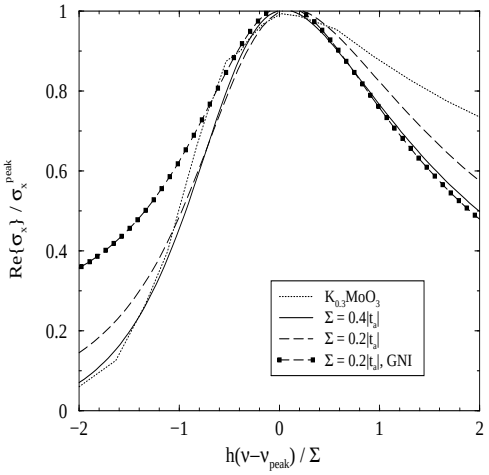

FIG. 2: The real part of the optical conductivity as a function of the damping energy Σ, for $|t_b| \to 0$, $\Delta_0 = 0.5|t_a|$, and $k_{\rm F} = 0.5\pi/a$. The filled squares illustrate the prediction of the usual, gauge-non-invariant (GNI) transverse model. The experimental data measured in $K_{0.3}MoO_3$ (Ref. [4]) are represented by the dotted line.

from two opposite effects, from this explicit temperature trend and from the implicit temperature dependence in $\Sigma(T)$ and/or $\Delta_0(T)$. The experimental data illustrating this competition, measured in various low-dimensional systems, can be found in Refs. [2, 5, 7], while a similar theoretical analysis is given in Ref. [9].

More importantly, this figure illustrates that the interband contribution vanishes for $\omega \to 0$, independently of $k_{\rm F}$. Such behaviour is due to the gauge-invariance factor $[\hbar\omega/E_{AS}(k_x)]^2$ in Eq. (13). The physical meaning of this observation is that in the metal-to-insulator phase transi-

tions (for example, for $k_F \to 0.5\pi/a$, $\Delta_0 \neq 0$) the dc conductivity has to vanish. The usual transverse approach, where the gauge-invariance factor is absent, gives, on the other hand, a finite $\sigma_x^{\rm dc}$ not only in the metallic regime, but also in the insulating regime (see Fig. 2 and an extensive discussion done in Ref. [8]). These conclusions are valid not only for the bond-energy-dimerization optical models, but also for the site-energy-dimerization optical models [11], as well as for the single-particle contributions to $\sigma_x^{\rm total}$ in the systems with CDW or SDW instabilities.

To compare briefly the predictions of the present model with experiments, we apply it now to the insulating $k_{\rm F} = 0.5\pi/a$ case, and, again, normalize the spectra. For the parameter $\Delta_0 = 0.5|t_a|$ describing the weak-splitting case, we obtain the results, shown in Fig. 2, which fit well the single-particle optical conductivity measured in the CDW ground state of $K_{0.3}MoO_3$. Notice that the usual transverse model (filled squares) significantly overestimates the subgap spectrum.

Finally, it should be recalled that the gauge invariant form of $\sigma_x^{\rm total}$ allows the consistent treatment of the conductivity sum rules [10]. For the lower band partially filled, the spectral weights of the intraband and total conductivity are given by

$$\begin{aligned} \frac{1}{2}\Omega^2_{\rm intra} &= \frac{2\pi e^2 n_x^{\rm eff}}{m}, \\ \frac{1}{2}\Omega^2_{\rm total} &= \frac{2\pi e^2}{m}\frac{1}{V}\sum_{\mathbf{k}\sigma}\gamma_{xx}^{SS}(\mathbf{k};2)f_S(\mathbf{k}), \end{aligned} \qquad (19)$$

respectively, and that of the interband contributions by $(1/2)(\Omega^2_{\rm total} - \Omega^2_{\rm intra})$. Moreover, the dc conductivity is directly related to the intraband spectral weight, according to the well-known relation $\sigma_x^{\rm dc} = \hbar\Omega^2_{\rm intra}/(4\pi\Sigma)$.

C. $|t_b| \to 0$, $T \to 0$ limit

The characterization of the low-frequency metallic response is intimately connected with the energy region between Σ_1 and $E_{AS}(k_{\rm F}) - \Sigma_2$ (see Fig. 1, for example). In general, in the weak-splitting optical models, both the Drude-like behaviour (characterized by $\mathrm{Re}\{\sigma_x(\omega)\} \propto \omega^{-2}$) and the non-Drude behaviour (where $\mathrm{Re}\{\sigma_x(\omega)\} \propto \omega^{-\alpha}, \alpha < 2$) are possible, as can be seen from Fig. 3, where the real part of the conductivity for various Fermi wave vectors is given.

A more detailed insight into the low-frequency response can be achieved from the doping dependence of $n_x^{\rm eff}$, which is shown in Fig. 4. The following conclusions are important: (i) The free-electron approximation (dashed curve) predicts the electronlike behaviour of the conduction electrons ($\partial n_x^{\rm eff}/\partial\delta > 0$) in the entire doping range $0 \le \delta \le 2$. (ii) The simple tight-binding model (dotted curve) leads to the electronlike regime for $0 \le \delta < 1$ and to the holelike regime ($\partial n_x^{\rm eff}/\partial\delta < 0$) for $1 < \delta \le 2$. (iii) The dimerized tight-binding model (solid curves) is characterized by the electronlike behaviour for $0 \le \delta < 1 - \delta_{\rm c}$ and $1 < \delta < 1 + \delta_{\rm c}$, and by the holelike behaviour for $1 - \delta_{\rm c} < \delta < 1$ and $1 + \delta_{\rm c} < \delta \le 2$. (iv) The non-Drude response is expected in the $1 - \delta_{\rm c} < \delta < 1 + \delta_{\rm c}$ doping region, i.e., where the spectral weight of the interband contributions becomes comparable to the intraband spectral weight.

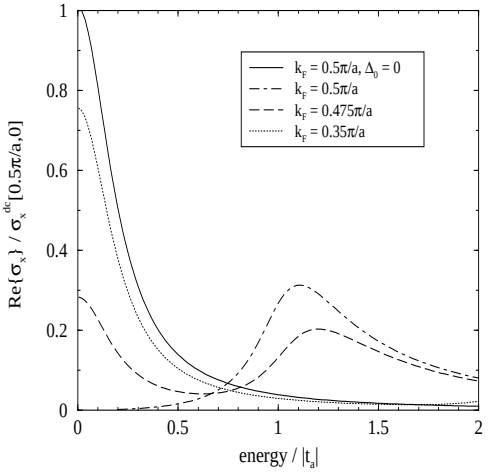

FIG. 3: The real part of the optical conductivity as a function of the Fermi wave vector, for $\Delta_0 = 0.5|t_a|$ and $\Sigma = 0.2|t_a|$. Here $\sigma_{\rm dc}(0.5\pi/a, 0)$ is the dc conductivity of the $k_{\rm F} = 0.5\pi/a$, $\Delta_0 = 0$ case.

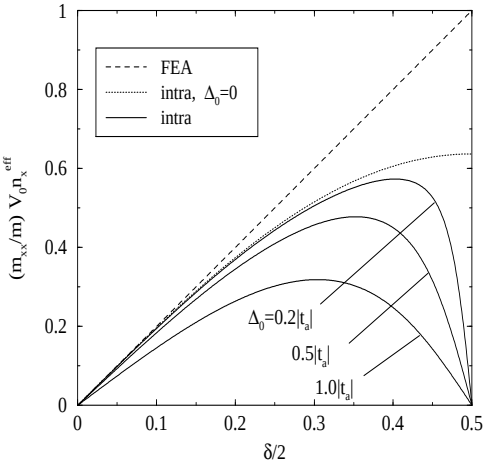

FIG. 4: The effective number of conduction electrons $V_0 n_x^{\rm eff}$ as a function of the electron doping $\delta = 2ak_{\rm F}/\pi$ (V_0 is the primitive cell volume). The prediction of the free-electron approximation (FEA) is also given for comparison.

For Δ_0 not to large, the critical doping $\delta_{\rm c}$ is proportional to Δ_0. Not surprisingly, for $1 - \delta_{\rm c} < \delta = 1 - \delta' < 1$ the electronic system would be described by the effective mass approximation which is given by

$$V_0 n_x^{\rm eff} = \frac{m}{m^*_{xx}}\delta' = -\frac{m}{m^*_{xx}}\delta + \frac{m}{m^*_{xx}} \qquad (20)$$

with δ' and m^*_{xx} representing, respectively, the number of doped holes (with respect to the half filling) and the

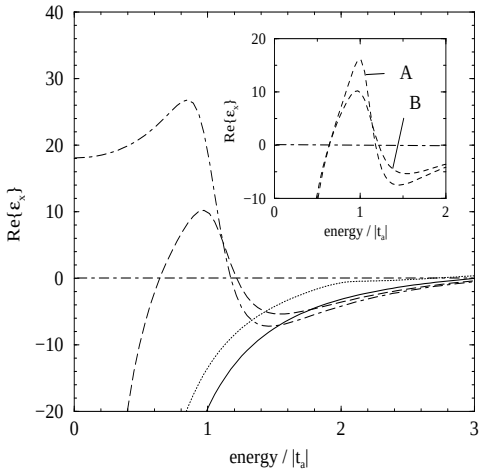

FIG. 5: Main figure: The dependence of the real part of the dielectric function on the Fermi wave vector, for $\Delta_0 = 0.5|t_a|$, $\hbar\sqrt{4\pi e^2/(V_0 m)} = 6|t_a|$, $\varepsilon_\infty = 2.5$, and $\Sigma = 0.2|t_a|$ (see the legend of Fig 3). Inset of figure: The influence of the damping energies on $\mathrm{Re}\{\varepsilon_x(\omega)\}$, for $k_\mathrm{F} = 0.475\pi/a$, $\Sigma = 0.12|t_a|$ (curve A), and $\Sigma = 0.2|t_a|$ (curve B).

effective mass of these holes. It must be noted that the effective mass m^*_{xx} is proportional now to Δ_0 and that in the limit $\Delta_0 \to 0$ this mass vanishes.

Finally, the real part of the dielectric function is affected by the dimerization in the way shown in Fig. 5. In the Drude regime the influence of the dimerization is negligible, giving only one zero-crossing of $\mathrm{Re}\{\varepsilon_x(\omega)\}$ placed at the frequency of the longitudinal intrachain ($q_y = 0$ in Eq. (18)) plasma mode. In the non-Drude regime two zeros of the dielectric function appear, describing the intrachain plasma oscillations, as well. The first frequency corresponds to the intraband plasma oscillations and the latter one to the total plasma oscillations. As illustrated in the inset of figure, in the underdamped regime ($\Sigma_i < \Delta_0$), considered in this article, the zeros of $\mathrm{Re}\{\varepsilon_x(\omega)\}$ are almost independent of the single-particle damping.

IV. CONCLUSION

In this paper we have studied the influence of the weak bond-energy dimerization on the optical properties of the Q1D systems, for the electron doping $0 \le \delta \le 1$. It is found that the gap parameter has the p_x symmetry. It is shown that the weak bond-energy dimerization leads to the dielectric function in which the local field corrections are negligible. The analysis reveals two different metallic states. First state corresponds to the usual electronlike Drude metal with the optical conductivity $\mathrm{Re}\{\sigma_x(\omega)\} \propto \omega^{-2}$, with the effective number of electrons characterized by $\partial n_x^{\mathrm{eff}}/\partial\delta > 0$ and only with one zero-point in $\mathrm{Re}\{\varepsilon_x(\omega)\}$. Second metallic state is the non-Drude state characterized by the $\omega^{-\alpha}$ behaviour of the low-frequency contribution to $\mathrm{Re}\{\sigma_x(\omega)\}$, where $\alpha < 2$. There are two zero-points in $\mathrm{Re}\{\varepsilon_x(\omega)\}$, and the effective number of electrons exhibits the holelike behaviour $\partial n_x^{\mathrm{eff}}/\partial\delta < 0$. The comparison with experimental data measured in various CDW systems shows good agreement for the single-particle contributions to the optical conductivity.

Acknowledgement

This work was supported by Croatian Ministry of Science under the project 119-204.

APPENDIX A: VERTEX FUNCTIONS

For the lower band partially filled and the upper band empty, relevant are the current vertices (again $r_{\beta x} = a$)

$$\begin{aligned} J_x^{SS}(k_x) &= J_x^0[\sin k_x a\cos\varphi(k_x) \\ &\quad -\frac{\Delta_0}{2|t_a|}\cos k_x a\sin\varphi(k_x)], \\ J_y^{SS}(k_x) &= J_y^0 \sin k_y b, \qquad \text{(A1)} \\ J_x^{SA}(k_y) &= \mathrm{i}J_x^0[\sin k_x a\sin\varphi(k_x) \\ &\quad +\frac{\Delta_0}{2|t_a|}\cos k_x a\cos\varphi(k_x)], \\ J_y^{SA}(k_y) &= 0, \qquad \text{(A2)} \end{aligned}$$

and the bare Raman vertices

$$\begin{aligned} \gamma_{xx}^{SS}(k_x;2) &= \gamma_{xx}^0[\cos k_x a\cos\varphi(k_x) \qquad \text{(A3)} \\ &\quad +\frac{\Delta_0}{2|t_a|}\sin k_x a\sin\varphi(k_x)], \\ \gamma_{yy}^{SS}(k_y;2) &= \gamma_{yy}^0\cos k_y b. \qquad \text{(A4)} \end{aligned}$$

Here $J_{x_i}^0 = e\hbar/(a_i m_{x_i x_i})$, $\gamma_{x_i x_i}^0 = m/m_{x_i x_i}$ and $m_{x_i x_i} = \hbar^2/(2|t_i|a_i^2)$ ($|t_i| \in \{|t_a|, |t_b|\}$, $a_i \in \{a, b\}$).

[1] C. S. Jacobsen, Low-Dimensional Conductors and Superconductors, D. Jérome and L. G. Caron (eds.), Plenum press, New York, 1986, p. 253.
[2] C. S. Jacobsen, D. B. Tanner and K. Bechgaard, Phys. Rev. B 28 (1983) 7019.
[3] L. Degiorgi, B. Alavi, G. Mihály and G. Grüner, Phys. Rev. B 44 (1991) 7808.
[4] L. Degiorgi, St. Thieme, B. Alavi, G. Grüner, R. H.

Mckenzie, K. Kim and F. Levy, Physics and Chemistry of Low-Dimensional Inorganic Conductors, C. Schlenker at al. (eds.), Plenum press, New York, 1996, p. 337.
[5] A. Schwartz, M. Dressel, G. Grüner, V. Vescoli, L. Degiorgi and T. Giamarchi, Phys. Rev. B 58, (1998) 1261.
[6] S. Uchida, T. Ido, H. Takagi, T. Arima, Y. Tokura, and S. Tajima, Phys. Rev. B 43 (1991) 7942.
[7] S. Lupi, P. Calvani, M. Capizzi, and P. Roy, Phys. Rev. B 62 (2000) 12 418.
[8] K. Kim, R. H. Mckenzie and J. W. Wilkins, Phys. Rev. Lett. 71 (1993) 4015.
[9] V. J. Emery and S. A. Kivelson, Phys. Rev. Lett. 71 (1993) 3701.
[10] I. Kupčić, cond-mat/0201387.
[11] I. Kupčić, unpublished.
[12] P. Županović, A. Bjeliš, and S. Barišić, Z. Phys. B 101 (1996) 387.
[13] S. A. Brazovskii, L. P. Gor'kov, and A. G. Lebed', Zh. Eksp. Teor. Fiz. 83 (1982) 1198 [Sov. Phys. JETP 56 (1982) 683].
[14] S. A. Brazovskii, I. E. Dzyaloshinskii, and S. G. Obukhov, Zh. Eksp. Teor. Fiz. 72 (1977) 1550 [Sov. Phys. JETP 45 (1977) 814].
[15] P. A. Lee, T. M. Rice and P. W. Anderson, Solid State Commun. 14 (1974) 703.
[16] G. Grüner, Density Waves in Solids, Addison-Wesley Publishing Company, New York, 1994, and references therein.
[17] D. Pines and P. Noziéres, The Theory of Quantum Liquids I, Addison-Wesley Publishing Co., Inc., New York, 1989.
[18] G. D. Mahan, Many-particle Physics, Plenum press, New York, 1990.
[19] A. A. Abrikosov and V. M. Genkin, Zh. Eksp. Teor. Fiz. 65 (1973) 842 [Sov. Phys. JETP 38 (1974) 417].
[20] I. Kupčić, Phys. Rev. B 61 (2000) 6994.